



**HAL**  
open science

## 5 GHz Lamb wave Wi-Fi channel filters

Alexandre Reinhardt, Marie Bousquet, Alice Joulie, Elisa Soulat, Catherine Maeder-Pachurka, Pierre Perreau, Grégory Enyedi, Gaël Castellan, Julien Delprato, Bruno Reig, et al.

► **To cite this version:**

Alexandre Reinhardt, Marie Bousquet, Alice Joulie, Elisa Soulat, Catherine Maeder-Pachurka, et al.. 5 GHz Lamb wave Wi-Fi channel filters. 2022 IEEE International Ultrasonics Symposium (IUS), Oct 2022, Venice, Italy. 2022, 10.1109/IUS54386.2022.9958311 . cea-04179300

**HAL Id: cea-04179300**

**<https://cea.hal.science/cea-04179300>**

Submitted on 9 Aug 2023

**HAL** is a multi-disciplinary open access archive for the deposit and dissemination of scientific research documents, whether they are published or not. The documents may come from teaching and research institutions in France or abroad, or from public or private research centers.

L'archive ouverte pluridisciplinaire **HAL**, est destinée au dépôt et à la diffusion de documents scientifiques de niveau recherche, publiés ou non, émanant des établissements d'enseignement et de recherche français ou étrangers, des laboratoires publics ou privés.

# 5 GHz Lamb wave Wi-Fi channel filters

Alexandre Reinhardt    Marie Bousquet    Alice Joulie    Elisa Soulat    Catherine Maeder-Pachurka  
*Univ. Grenoble Alpes,    Univ. Grenoble Alpes,    Univ. Grenoble Alpes,    Univ. Grenoble Alpes,    Univ. Grenoble Alpes,*  
*CEA, LETI,    CEA, LETI,    CEA, LETI,    CEA, LETI,    CEA, LETI,*  
Grenoble, France    Grenoble, France    Grenoble, France    Grenoble, France    Grenoble, France  
alexandre.reinhardt@cea.fr

Pierre Perreau    Grégory Enyedi    Gaël Castellan    Julien Delprato    Bruno Reig  
*Univ. Grenoble Alpes,    Univ. Grenoble Alpes,    Univ. Grenoble Alpes,    Univ. Grenoble Alpes,    Univ. Grenoble Alpes,*  
*CEA, LETI,    CEA, LETI,    CEA, LETI,    CEA, LETI,    CEA, LETI,*  
Grenoble, France    Grenoble, France    Grenoble, France    Grenoble, France    Grenoble, France

Jean-Luc Thomassin    Hossein Alavi    Paul Fischer  
*Univ. Grenoble Alpes    Intel Corporation    Intel Corporation*  
*CEA, IRIG    Hillsboro OR, United States    Hillsboro OR, United States*  
Grenoble, France

**Abstract**—Lamb-wave resonators offer the possibility to adjust their resonance frequency by varying the period of their interdigitated electrodes. Leveraging the high frequency operation of the first antisymmetric mode in thin film lithium niobate membranes, this opens perspectives towards the cointegration of several filters operating in the 4–7 GHz range on the same die. To demonstrate this, we designed and fabricated a set of channel filters for the 5 GHz Wi-Fi standard. Resonators exhibit frequencies varying from 5.1 to 5.6 GHz and electromechanical coupling ranging from 5.5 to 9% for electrodes pitches varying from 1.1  $\mu\text{m}$  to 800 nm, with quality factors in the 400–600 range. 3 and 5-resonator ladder filters exhibit insertion losses close to 2 (resp. 4) dB and rejection of 20 (resp. 30) dB, mostly limited by the frequency positioning of the resonators and feedthrough capacitances.

**Index Terms**—Lamb wave, LiNbO<sub>3</sub>, Wi-Fi, filters

## I. INTRODUCTION

In the past few years, resonators and filters based on single-crystal lithium niobate (LiNbO<sub>3</sub>) or lithium tantalate thin films have raised a strong interest. Layered Surface Acoustic Wave (SAW) devices based on such films have demonstrated unprecedented performances in terms of operation frequency, electromechanical coupling factors, quality factors and temperature coefficients of frequency, up to the point of being dubbed Incredibly High Performance SAW (IHP-SAW) [1]. To keep the SAW confined in the thin piezoelectric film, its velocity has to be limited by the bulk wave velocities in the underlying substrate. This relaxes photolithographic requirements compared to classical SAW devices, but still makes frequencies above 3 GHz challenging to reach, even with projection lithography. A solution to lift this limitation is to insert an acoustic Bragg

This work has been performed with the help of the “Plateforme Technologique Amont de Grenoble”, with the financial support of the “Nanosciences aux limites de la Nanoélectronique” Foundation and CNRS Renatech network.

mirror between the piezoelectric film and the substrate, so as to ensure a proper confinement independently of substrate characteristics. This allows exploiting quasi longitudinal waves with a significantly faster phase velocity. Doing so, Kimura *et al.* demonstrated a 5 GHz Longitudinal Leaky SAW (LLSAW) resonator operating at 5 GHz with an electrode pitch of 600 nm [2], which is still challenging to reach with conventional photolithography equipments.

On the other hand, Bulk Acoustic Wave (BAW) resonators and filters are more suited towards operation at high frequency, since they exploit a thickness mode of the piezoelectric film. Historically, AlN was the reference material for these devices [3]. The need for larger electromechanical coupling factors has caused a move to Al<sub>1-x</sub>Sc<sub>x</sub>N [4]. However, because of the reliance on a thickness bulk mode, these devices lack flexibility when it comes for cointegrating several filters on the same die.

Eventually, Lamb-wave resonators based on piezoelectric thin films exhibit some unique characteristics. The initial devices, based on AlN, only reached electromechanical factors of at most 2% [5], [6]. Many efforts have focused on investigating new configurations promoting electromechanical coupling factors approaching, or even beyond the electromechanical coupling factors of BAW resonators [7]. However, it is only with the adoption of single crystal films, usually lithium niobate, that really large electromechanical coupling factors, up to 55%, could be achieved [8]. Initially, fundamental shear plate (SH<sub>0</sub>) [8] or symmetric modes (S<sub>0</sub>) [9] were exploited, leading to operation below 1 GHz. Higher frequencies, up to 5 GHz, were reached by exploiting the first-order antisymmetric mode (A<sub>1</sub>) mode in Z-cut LiNbO<sub>3</sub> membranes [10], [11]. For such a mode, frequency is defined primarily by the thickness of the piezoelectric film or the membrane, similarly to a BAW device [12]. However, the dispersive nature of this mode

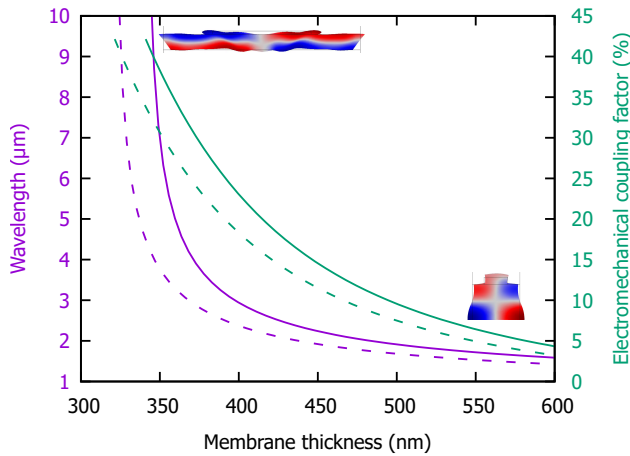


Fig. 1: Dispersion characteristics for the  $A_1$  mode in a Z-cut  $\text{LiNbO}_3$  membrane, propagation Y: wavelength needed to reach a frequency of 5.25 GHz (continuous) and 5.57 GHz (dashed) and corresponding electromechanical coupling factor as a function of the membrane thickness. The metal thickness is assumed to be 20% of the membrane thickness, with a metallization ratio  $a/p$  of 0.5. The insets illustrate the mode shapes for a single period for the two ends of the curves.

allows tuning the operation frequency by a proper selection of the wavelength. This offers thus, in principle, possibilities towards the cointegration of several filters.

To demonstrate this capability, we designed and fabricated a set of filters targeting the 5 GHz Wi-Fi 160 MHz channel bands. Unlike previously reported filters using  $A_1$  Lamb waves in lithium niobate thin films, operating in a similar frequency range, which focused on relatively large bandwidth filters (12.7%) [13], we consider here more modest bandwidths (3% relative bandwidth), putting the emphasis on the cointegration of two filters. Sections II – IV will respectively detail the design of these two filters, their fabrication, and their characterization.

## II. WI-FI CHANNEL FILTERS DESIGN

The  $A_1$  Lamb mode has a hybrid nature: it is close to a bulk mode in the vicinity of its cutoff frequency but exhibits a higher degree of lateral propagation away from it. This allows fixing the resonance frequency by a combination of the membrane thickness and the selected wavelength. Fig. 1 shows (violet curves) possible combinations to reach the center frequencies of the desired filters. Along these curves, one can also notice that the electromechanical coupling factor decreases with increasing thickness to wavelength ratio ( $h/\lambda$ ). Thus, to reach the electromechanical coupling factors in the 6–9% needed to synthesize the channel filters, an ideal membrane thickness of 500 nm and wavelengths close to 2  $\mu\text{m}$  are necessary.

These figures were refined by periodic finite element simulations of the resonator structures. The harmonic admittance calculations shown in Fig. 2 confirm that a correct positioning of the resonance and antiresonance frequencies of the series and parallel resonators of the two filters is achieved for electrode pitches of respectively 0.82, 0.88, 0.93 and 1.02  $\mu\text{m}$  (assuming metallization ratios  $a/p$  of 0.5 in each case). It is noteworthy

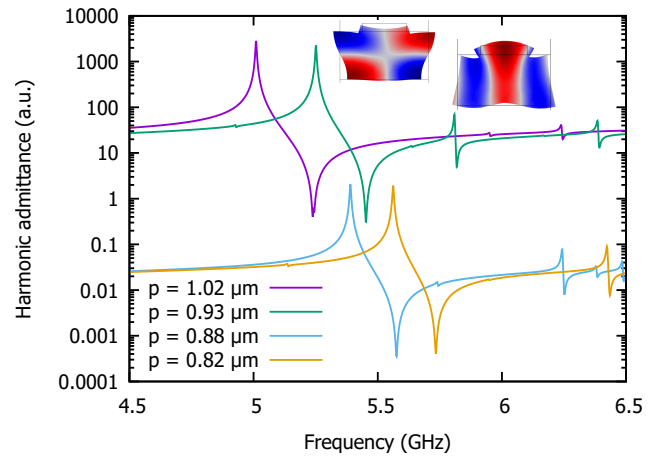


Fig. 2: Harmonic admittance for the  $A_1$  mode in a 500 nm-thick Z-cut  $\text{LiNbO}_3$  membrane, propagation Y, with 90 nm-thick aluminum electrodes and a metallization ratio  $a/p$  of 0.5, for the four electrodes pitches suitable to implement the series and parallel resonators of the two channel filters. Insets are the mode shapes for a single period for the main resonance and the closest spurious resonance, from the calculation with  $p = 930$  nm. Colors represent the horizontal (resp. vertical) displacement component for the mode shape at resonance (resp. first spurious resonance).

that some spurious resonances appear above 5.7 GHz. They are apparently similar to those also reported in previous works by others [12], [13], which described them as overtones of the  $A_1$  mode. Here, the insets in Fig. 2 indicates that the spurious mode rather corresponds to the fourth lateral overtone of the  $A_0$  mode. Despite this mode being relatively slow (circa 2200 m/s), the small pitch values bring its fundamental resonance close to 1.2 GHz, and thus its fourth overtone in the frequency range of interest. This is confirmed by the observation on Fig. 2 that when reducing electrodes pitches to 880 and 820 nm, this spurious resonance is pushed to the 6.2–6.5 GHz range. Since this mode is sensitive to the metallization, we adjusted the aluminum thickness to 90 nm to position this resonance out of the filter bandwidths, but we could not completely suppress it.

The calculated harmonic admittances allow for the extraction of propagation parameters for the Lamb wave of interest. The effective wave velocities were found to vary from 11,400 to 14,000 m/s, depending on the electrodes periodicity. Such large values are related to a still near-vertical propagation of the wave. This is also confirmed by the limited mechanical couplings between adjacent electrodes, which manifest by strong internal reflections inside a transducer. As a consequence, we could design relatively compact resonators. The smallest series resonators needed only a few tens of electrodes, including reflectors, to obtain decent electric responses. Fig. 3 shows the simulated responses of the two filters using either a Butterworth-Van Dyke model (dashed) or a full 2D finite element simulation used to validate the design of each resonator structure. In each case, arbitrary losses were included in the model, to reach quality factors of about 500. The finite element model reveals that the overtone of the  $A_0$  mode

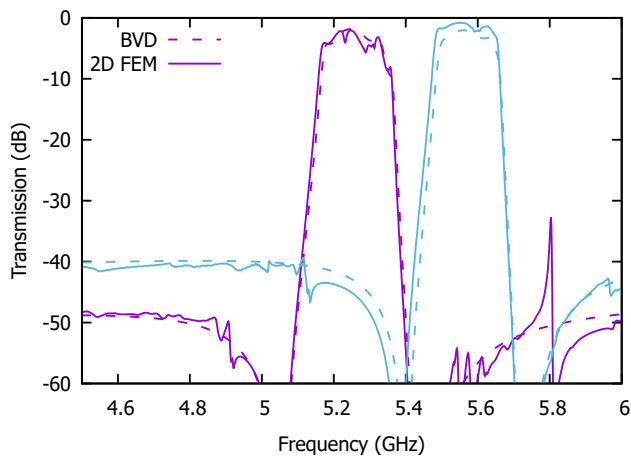


Fig. 3: Simulated filter responses: comparison of the responses calculated using a BVD model (dashed) and a 2D finite element simulation (solid) for a 5-resonators ladder filter.

discussed above manifests as a spurious resonance appearing at 5.8 GHz, for the lowest frequency filter, and limits the out of band rejection, but has otherwise no critical influence. So for the sake of this study, we did not look further into suppressing it. The other spurious contributions, particularly visible on the lowest frequency filter induce some additional in-band ripple. Before trying to mitigate these contributions, we went on fabricating a first set of filters.

### III. FILTERS FABRICATION

The fabrication of the Lamb wave filters follows the process flow for the fabrication of LiNbO<sub>3</sub> BAW resonators described in [14], adapted to the peculiarities of Lamb wave devices. A Z-cut LiNbO<sub>3</sub> wafer is ion implanted to define a weak subsurface interface. A sacrificial layer made of amorphous silicon is then deposited by sputtering and patterned by dry etching. Silicon dioxide is then deposited and polished to provide a smooth surface compatible with wafer bonding. This wafer is then bonded onto another Z-cut LiNbO<sub>3</sub> wafer coated with silicon dioxide. A subsequent thermal annealing strengthens the bonding and leads to the implanted wafer to split, leaving only a thin piezoelectric film attached to the carrier wafer. This film is polished to smooth its surface left rough by the splitting and to adjust its thickness to 500 nm. A set of alignment marks are formed by lift-off of an evaporated platinum layer. Aluminum electrodes are then sputtered. Although the resolution of the interdigitated electrodes remains accessible to UV- or DUV- projection lithography, we opted here for ebeam lithography. The aluminum layer was then etched by ion beam etching. Release holes were formed by photolithography and ion beam etching of the lithium niobate film. Eventually, the membranes are released by etching the amorphous silicon sacrificial layer with gaseous XeF<sub>2</sub>.

Fig. 4 shows an optical microscope view of one of the filters fabricated. The membranes exhibit no cracks or defects after release, only some slight bending due to residual stress

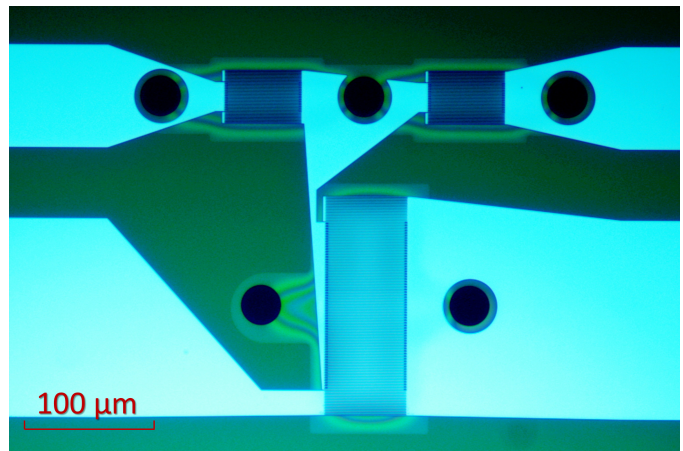


Fig. 4: Optical microscope image of a T-stage ladder filter.

in the lithium niobate and aluminum films, noticeable by the appearance of interference fringes around the resonators.

### IV. CHARACTERIZATION

The fabricated resonators and filters have been then probed directly on wafer using coplanar Ground-Signal-Ground probes connected a Vector Network Analyzer (VNA), after a conventional Short-Open-Load-Thru calibration. The responses of standalone versions of the resonators included in the filter circuits are shown Fig. 5a without deembedding. As expected, their resonance frequencies vary from 5.1 to 5.6 GHz, for the various electrode pitches. The corresponding electromechanical coupling factors vary from 8.9 to 5.5%, following a trend close to the theoretical variation of coupling factor with  $h/\lambda$ . Quality factors at antiresonance, for devices with an antiresonance not disturbed by spurious contributions, are evaluated in the 400-600 range. This is similar to previously reported work by other groups [13]. The best resonators exhibit impedance ratios up to 430.

A comparison with the initial resonator simulations indicate that the pitch-frequency dependency is in reasonable agreement for most of the resonators, except for small frequency shifts in the range of 60 MHz for the resonators with pitches of 820 and 880 nm. Resonators with a pitch of 1020 nm nearly match their expected antiresonance frequency, although an unexpected spurious resonance at 5 GHz shifts their resonance frequency. These shifts could be attributed to slight deviations from expected thicknesses for the LiNbO<sub>3</sub> and Al layers, inaccuracies in the elastic properties of the aluminum films, and to some overetch of the interdigitated electrodes, which affects more strongly the devices with the smallest electrode dimensions. For reasons not yet clarified, the resonators with an electrode pitch of 930 nm exhibit a significant frequency shift compared to the initial design. This affects dramatically the lowest frequency filter whose transmission, shown in Fig. 5b, is badly distorted.

On the other hand, the highest frequency filter exhibits a more conventional filter response. Despite its bandwidth being reduced due to a different frequency misalignment of

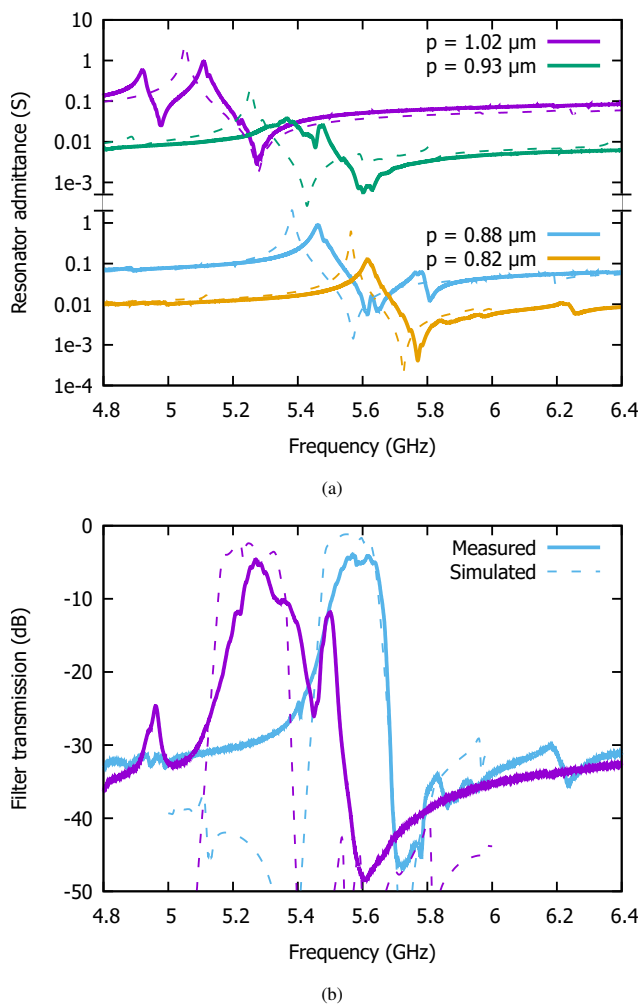


Fig. 5: Resonators (a) and filters (b) measurements (solid lines) and comparison with initial simulations (dashed lines).

the series and parallel resonators, and some additional in-band ripple appearing due to a spurious resonance affecting the antiresonance of the parallel resonators, it exhibits 4 dB insertion losses for a 5-resonators filter (resp. 2 dB losses for a 3-resonators filter) and rejections of -30 dB (resp. -20 dB) far from the passband. Again, these rejections are lower than those expected from Fig. 3. It must however be mentioned that the initial designs did not include electromagnetic simulations, and do therefore not account for parasitic feedthrough capacitances or other effects.

## V. CONCLUSIONS

We have designed and fabricated two bandpass filters with center frequencies of respectively 5.25 and 5.57 GHz, leveraging the flexibility offered by the  $A_1$  Lamb-wave mode in Z-cut  $\text{LiNbO}_3$  membranes to adjust resonators frequency by varying their interdigitated electrodes pitch from 820 to 1020 nm. The fabricated resonators exhibit electromechanical coupling factors between 5.5 and 8.9%, and quality factors in the 400-600 range. Despite issues related to spurious resonances

and frequency misalignments, functional filters exhibit 4 dB insertion losses and -30 dB insertion losses, respectively limited by resistive losses and capacitive feedthrough. Although the filter responses themselves need to be improved, we have demonstrated the possibility to implement two filters with center frequencies spaced from at least 10%.

Future work will aim at improving the models to improve the relative frequency positioning of the resonators, reducing the spurious resonances brought by other Lamb wave modes, and improve filter designs to include spurious electromagnetic effects that become prominent at those frequencies.

## REFERENCES

- [1] T. Takai, H. Iwamoto, Y. Takamine, H. Yamazaki, T. Fuyutsume, H. Kyoya, T. Nakao, H. Kando, M. Hiramoto, T. Toi, M. Koshino, and N. Nakajima, "Incredible high performance SAW resonator on novel multi-layered substrate," in *Proceedings of the 2016 IEEE International Ultrasonics Symposium*.
- [2] T. Kimura, M. Omura, Y. Kishimoto, H. Kyoya, M. Mimura, H. Okunaga, and K.-y. Hashimoto, "A high velocity and wideband SAW on a thin  $\text{LiNbO}_3$  plate bonded on a Si substrate in the SHF range," in *Proceedings of the 2019 IEEE International Ultrasonics Symposium*, pp. 1239–1248.
- [3] R. Ruby, "A decade of FBAR success and what is needed for another successful decade," in *Proceedings of the 2011 Symposium on Piezoelectricity, Acoustic Waves and Device Applications*, pp. 365–369.
- [4] R. Aigner, G. Fattinger, M. Schaefer, K. Karnati, R. Rothemund, and F. Dumont, "BAW filters for 5G bands," in *Proceedings of the 2018 IEEE International Electron Devices Meeting*, pp. 14.5.1–14.5.4.
- [5] J. Bjurström, I. Katardjiev, and V. Yantchev, "Lateral-field-excited thin-film lamb wave resonator," *Applied Physics Letters*, vol. 86, no. 15, p. 154103, 2005.
- [6] A. Volatier, G. Caruyer, D. Tanon, P. Ancey, E. Defay, and B. Dubus, "UHF/VHF resonators using lamb waves co-integrated with bulk acoustic wave resonators," in *Proceedings of the 2005 IEEE Ultrasonics Symposium*, vol. 2, pp. 902–905.
- [7] Y. Zhu, N. Wang, C. Liu, and Y. Zhang, "A review of the approaches to improve the effective coupling coefficient of AlN based RF MEMS resonators," in *Proceedings of the 2020 Joint Conference of the IEEE International Frequency Control Symposium and International Symposium on Applications of Ferroelectrics*.
- [8] J. Zou, V. Yantchev, F. Iliev, V. Plessky, S. Samadian, R. B. Hammond, and P. J. Turner, "Ultra-large-coupling and spurious-free  $\text{SH}_0$  plate acoustic wave resonators based on thin  $\text{LiNbO}_3$ ," *IEEE Trans. Ultrason., Ferroelectr., Freq. Control*, vol. 67, no. 2, pp. 374–386, 2020.
- [9] F. V. Pop, A. S. Kochhar, G. Vidal-Álvarez, and G. Piazza, "Investigation of electromechanical coupling and quality factor of X-cut lithium niobate laterally vibrating resonators operating around 400 MHz," *J. Microelectromech. Syst.*, vol. 27, no. 3, pp. 407–413, 2018.
- [10] M. Kadota, T. Ogami, K. Yamamoto, Y. Negoro, and H. Tochishita, "High-frequency Lamb wave device composed of  $\text{LiNbO}_3$  thin film," *Japanese Journal of Applied Physics*, vol. 48, no. 7, p. 07GG08, jul 2009.
- [11] Y. Yang, R. Lu, L. Gao, and S. Gong, "A C-band lithium niobate MEMS filter with 10% fractional bandwidth for 5G front-ends," in *Proceedings of the 2019 IEEE International Ultrasonics Symposium*, pp. 1981–1984.
- [12] V. Plessky, S. Yandrapalli, P. J. Turner, L. G. Villanueva, J. Koskela, M. Faizan, A. De Pastina, B. Garcia, J. Costa, and R. B. Hammond, "Laterally excited bulk wave resonators (XBARs) based on thin lithium niobate platelet for 5GHz and 13 GHz filters," in *Proceedings of the 2019 IEEE MTT-S International Microwave Symposium*, 2019, pp. 512–515.
- [13] P. Turner, B. Garcia, V. Yantchev, G. Dyer, S. Yandrapalli, L. Villanueva, R. Hammond, and V. Plessky, "5 GHz band n79 wideband microacoustic filter using thin lithium niobate membrane," *Electronics Letters*, vol. 55, no. 17, pp. 942–944, 2019.
- [14] A. Reinhardt, M. Bousquet, A. Joulie, C.-L. Hsu, F. Delaguiillaume, C. Maeder-Pachurka, G. Enyedi, P. Perreau, G. Castellan, and J. Lugo, "Lithium niobate film bulk longitudinal wave resonator," in *Proceedings of the 2021 Joint Conference of the European Frequency and Time Forum and IEEE International Frequency Control Symposium*.